

UC Irvine

UC Irvine Previously Published Works

Title

Hydrogenation catalyst generates cyclic peptide stereocentres in sequence

Permalink

<https://escholarship.org/uc/item/6rb4h4z3>

Journal

Nature Chemistry, 10(9)

ISSN

1755-4330

Authors

Le, Diane N
Hansen, Eric
Khan, Hasan A
et al.

Publication Date

2018-09-01

DOI

10.1038/s41557-018-0089-5

Peer reviewed



Published in final edited form as:

Nat Chem. 2018 September ; 10(9): 968–973. doi:10.1038/s41557-018-0089-5.

Hydrogenation Catalyst Generates Cyclic Peptide Stereocenters in Sequence

Diane N. Le¹, Eric Hansen², Hasan A. Khan^{1,3}, Byoungmoo Kim^{1,3}, Olaf Wiest^{2,4}, Vy M. Dong¹

¹Department of Chemistry, University of California, Irvine, California 92697, USA

²Department of Chemistry and Biochemistry, University of Notre Dame, Notre Dame, Indiana 46556, USA

³Department of Chemistry, University of Toronto, 80 St. George Street, Toronto, Ontario M5S 3H6, Canada

⁴Lab of Computational Chemistry and Drug Design, School of Chemical Biology and Biotechnology, Peking University, Shenzhen, China

Abstract

Molecular recognition plays a key role in enzyme-substrate specificity, the regulation of genes, and the treatment of diseases. Here we demonstrate how a synthetic catalyst can selectively bind a dehydroamino acid residue to initiate a sequential and stereoselective synthesis of cyclic peptides. Our combined experimental and theoretical study reveals the underpinnings of a cascade reduction that occurs with high stereocontrol and in one direction around a macrocyclic ring. This mechanistic insight provides a foundation for the use of cascade hydrogenations.

Through the art of synthesis, chemists build simplified models to understand how information encoded in molecules can be used to control chemical processes.^{1–3} One example of this in nature is the ribosome,^{4–6} which recognizes a specific start codon in the mRNA strand and catalyzes the sequential synthesis of a peptide in the *N* to *C* direction (Fig. 1a).⁷ This flow of sequence-specific information is encoded by sets of nucleic acids.⁸ In a study in supramolecular chemistry, Leigh and coworkers synthesized an artificial small-molecule machine that synthesizes polypeptides with directionality.⁹ Leigh's machine features a stoichiometric amount of thiol that moves along the rotaxane to construct a hexapeptide in the *C* to *N* direction (Fig. 1b). In contrast, we herein describe a rhodium-catalyst that promotes a cascade reduction to construct a cyclic peptide in the *C* to *N* direction. This catalyst can recognize information encoded in a sequence of prochiral units, to create a cyclic peptide via hydrogenation, with excellent levels of stereocontrol (Fig. 1c).

Correspondence to: dongv@uci.edu, owiest@nd.edu.

Author Contributions

D.N.L., H.A.K., and B.K. performed the chemical reactions. E.H. conducted the computational experiments. All authors contributed to the writing and editing of the manuscript.

Data availability statement

Full experimental procedures and spectral data for all new compounds as well as computational details are included in the Supplementary Information and are available from the corresponding authors on request.

On the basis of combined experimental and theoretical studies, we provide evidence for a unique mechanism that involves unidirectional reduction to set four stereocenters around the macrocyclic ring. Our study also provides a blueprint for using cascade catalysis¹⁰ in building cyclic peptides.

Cyclic peptides have attracted attention as therapeutics^{11,12} due to their enhanced metabolic stability,¹³ conformational rigidity,¹⁴ and potential to mimic protein–protein interactions.¹⁵ As a result, these circular structures continue to inspire the invention of synthetic tools and strategies.¹⁶ The classic approach relies on coupling chiral, enantiopure amino acid building blocks to generate a linear peptide prior to ring-closing.¹⁷ However, valuable enantiopure linear peptides are often affected at the macrocyclization step, suffering from *C* terminal epimerization and competing oligomerization.¹⁸ In contrast, we imagined first constructing a dehydropeptide using achiral building blocks. On the basis of previous studies, this linear dehydropeptide should readily ring-close to generate a macrocycle more efficiently than its saturated counterpart.¹⁹ In addition to the advantage of efficient ring-closing, a transition metal catalyst could be used to achieve a unidirectional cascade hydrogenation to furnish the requisite stereogenic centers in a single step.

Results and Discussion:

In accordance with this blueprint, we prepared the linear pentapeptide **4** containing four dehydrophenylalanines (Phe) from oxazolone **1** using a modified version of Bergmann's peptide synthesis.²⁰ The two-step peptide elongation involves isolable oxazolone **1** as an activated form of carboxylic acid, which could ring-open in the presence of an amine nucleophile such as racemic β -phenylserine to form **2**. Then, the resulting peptide is activated with sodium acetate and acetic anhydride to afford an elongated oxazolone **3** (Fig. 2a). Following these iterations, we obtained the linear pentapeptide **4** in 53% yield over six steps. After deprotection of linear precursor **4** using TFA, DMAP was added as a nucleophilic catalyst to facilitate aminolysis to afford the corresponding cyclic dehydropeptide **5a** in 81% yield over two steps with no dimerization observed, despite the relatively high concentration (0.1 M) (Fig. 2b).

To provide a more convenient handle for NMR analysis, we also prepared fluorinated analogue **5a'** (Supplementary Information). Considering that there are four dehydroamino acid residues in **5a'**, full reduction could generate a total of sixteen possible stereoisomers. Surprisingly, when a combination of [Rh(cod)₂]BF₄ and an achiral ligand (dppp) was used as a catalyst, one diastereomer was formed in 88% yield and with excellent diastereocontrol (20:2:1:1:1 *dr*) (Fig. 3, right). Through independent synthesis from D- and L-phenylalanine, we confirmed that this isomer was (\pm) cyclic D,L- α -peptide **6a'**. Of note, cyclic D,L- α -peptides have been used as therapeutic agents against gram negative and gram positive bacteria.^{21,22} In stark contrast, Pd/C produced a racemic mixture of all eight possible diastereomers ((\pm)-**6a-h'**), which were detected by ¹⁹F-NMR spectroscopy (Supplementary Fig. 5).

The Rh-catalyzed hydrogenation of enamides is an irreversible process.²³ Thus, the essentially complete diastereoselectivity observed in the presence of a simple, achiral ligand

(*i.e.* dppp) suggests that this reduction perhaps is proceeding in a specific order about the macrocyclic ring and is controlled by the sequence of the substrate. This observation in turn implies that the hydrogenation is initiated by recognition of the Rh-catalyst to a specific dehydrophenylalanine. To understand the intriguing finding, we performed further experimental and theoretical studies of the mechanism.

First, we tested the hypothesis of a strictly sequential reduction. If the hydrogenation proceeds in one direction around the ring starting with a specific dehydrophenylalanine (**1**, Fig. 4a), three intermediate macrocycles would arise (such as (\pm)-**5b'**, (\pm)-**5c'**, and (\pm)-**5d'**). By stopping the reduction of cyclic peptide **5a'** at various time points, three distinct intermediates were observed by ^{19}F -NMR spectroscopy. Next, we independently prepared and characterized cyclic peptides **5b'**, **5c'**, and **5d'**. The spectroscopic data for these three structures matched the structure of the aforementioned intermediates by ^{19}F -NMR. Moreover, when intermediate **5b'** was subjected to the Rh-catalyzed hydrogenation conditions, the corresponding cyclic peptide **6a'** was obtained in 76% yield and 20:<1:<1:<1:<1 *dr* (Fig 4b). Similarly, when we subjected cyclic peptide **5c'** to hydrogenation, we also observed cyclic peptide **6a'** in 99% yield and 20:<1:<1:<1:<1 *dr*. Finally, hydrogenating cyclic peptide **5d'** gave the desired peptide in 99% yield and 20:<1:<1:<1:<1 *dr*. Together, these experiments support the proposed intermediates that arise during a sequential reduction that occurs with high *anti* diastereoselectivity.

Next, we studied the structural origin of the experimentally observed *anti* selectivity through theoretical studies. Given the complexity of cyclic dehydropeptide **5a** (Fig. 2), even a minimal conformational analysis of the transition state is not feasible. We therefore used the transition state force field (TSFF) for the Rh-catalyzed hydrogenation of enamides,²⁴ which we developed previously using the quantum guided molecular mechanics (Q2MM) method.²⁵ This method was previously shown to allow the rapid exploration of the conformational space at the transition state using Monte Carlo sampling, and by Boltzmann averaging of the relative energies of the conformational ensembles of the diastereomeric transition structures, to accurately predict the stereochemistry of the hydrogenation.²⁶

Figure 5 summarizes the results of these simulations for the cyclic dehydropeptide **5a** using $[\text{Rh}(\text{dppp})]^+$. Figure 5a and 5b shows the lowest energy transition structures **7a[‡]** and **7s[‡]** for the hydrogenation of cyclic dehydropeptide **5b** leading to the *anti* (left) and *syn* (right) diastereoselectivity, respectively. The accessible conformational space of the cyclic dehydropeptide is complex, and no single conformation or interaction is solely responsible for the calculated and experimentally observed preference. Nevertheless, analysis of the conformations of **7a[‡]** and **7s[‡]** shows that the side chains at Phe₁ and APhe₂ are positioned in a pseudo-equatorial position to minimize steric repulsion with the dppp ligand, while maximizing the π -stacking between the phenyl rings (Supplementary Fig. 18), and thus the backbone of the cyclic dehydropeptide is distorted into a strained conformation. As a result, one amide bond in **7s[‡]** is forced into an energetically unfavorable²⁷ *cis* conformation (highlighted in green, Fig. 5b), favoring the transition structure leading to the observed *anti* selective hydrogenation. Clustering of the low-energy transition structures also shows that the transition structures for the hydrogenations at Phe₃ and Phe₄ leading to the

experimentally observed product are stabilized by more intramolecular hydrogen bonds (Supplementary Fig. 9-11).

Moreover, after the first hydrogenation at Phe₁ in cyclic dehydropeptide **5a**, the subsequent reductions occur *anti* with predicted selectivities ranging from 30:1 to 78:1 *dr* (Fig. 5c), in good agreement with the experimentally observed diastereoselectivity of 20:<1:<1:<1:<1 (cf Fig. 3 and 4). It is noteworthy that the final hydrogenation at Phe₄ is the least selective one, suggesting that the diastereoselectivity is related to the increased flexibility of the cyclic dehydropeptide **5d**.

The computational studies also allow us to probe the basic hypothesis of a sequential, unidirectional hydrogenation controlled by the interplay between the substrate and Rh catalyst. Figure 5d shows the results for the expected diastereoselectivity for the second hydrogenation at the three possible centers. Only the simulations for the sequential hydrogenation at Phe₂ leads to the experimentally observed result, while reaction at Phe₃ or Phe₄ would lead to significantly different or even opposing diastereoselectivities. Together, the experimental and computational results demonstrate that the Rh catalyst preferentially binds to Phe₁ for the initial reduction of cyclic dehydropeptide **5a**. We hypothesize that the adjacent glycine residue, containing a sp³-hybridized α -carbon, enables the flexibility for the Rh catalyst to bind to Phe₁ in a reactive conformation to initiate the sequential reduction.²⁸ As the hydrogenation proceeds in the *C* to *N* direction to furnish a new α -substituted stereocenter, the next Phe in the sequence becomes more flexible and is hydrogenated in the subsequent step. The opposite *N* to *C* direction is disfavored for the initial reduction because the reactive conformations of Phe₄ are higher in energy than for Phe₁ (Supplementary Fig. 22).

Finally, we studied the question of whether an appropriate chiral ligand can override the diastereoselectivity observed when using the Rh-dppp catalyst. Among the thousands of chiral phosphine ligands developed for asymmetric hydrogenation,²⁹ Duanphos is the best for reduction of α -(acetamido)acrylate derivatives.³⁰ We previously used Duanphos to access cyclic peptides by overriding substrate bias in the synthesis of the chickweed natural product, dichotomin E.¹⁹ With 5 mol% [Rh(cod)₂]BF₄, (*R,R'*,*S,S'*)-Duanphos gave cyclic peptide **6b** in 86% isolated yield and >99% *ee* (Fig. 6a). This Rh-catalyst overcomes any substrate bias to generate a single stereoisomer with 20:<1 *dr* as observed by ¹⁹F-NMR spectroscopy (Supplementary Information). In analyzing the transformation by both ¹⁹F-NMR and MS analysis at an early timepoint, we observe the formation of only two unsaturated intermediates, thus supporting a mechanism involving sequential reduction (Supplementary Information). Subsequently, we also synthesized cyclic dehydropeptide **8** containing dehydroleucine and subjected it to the Rh-Duanphos catalyst to afford cyclic peptide **9a** in 84% yield, >99% *ee*, and 20:<1 *dr* (Fig. 6b). In using the Rh-Duanphos catalyst with our cyclic dehydropeptides, we are able to extend the cascade hydrogenation to afford access to cyclic peptides with high levels of enantio- and diastereocontrol.

Conclusion:

Molecular recognition between transition metal catalysts and amino acids is a powerful strategy in organic synthesis.³¹ Through our combined experimental and theoretical study, we have demonstrated the first example of a unidirectional hydrogenation controlled by a small synthetic peptide and Rh catalyst. The catalyst most likely dissociates from the peptide, and thus the *C* to *N* directionality in the hydrogenation is controlled by catalyst-substrate recognition, as opposed to processive mechanisms where the catalyst remains bound to the substrate.³² Studying the mechanism of Rh-catalyzed hydrogenation has provided insights with far-reaching impact in catalysis, such as enantioselective control (Knowles and Noyori),^{33,34} Curtin-Hammett selectivity (Halpern),²³ and chiral amplification (Kagan).^{35,36} In the context of hydrogenation, our report showcases the first example of a sequential and stereoselective mechanism. These insights highlight the potential of molecular recognition in organic synthesis and provides a foundation for the construction of cyclic peptides by cascade catalysis.¹⁰

Supplementary Material

Refer to Web version on PubMed Central for supplementary material.

Acknowledgements

Funding was provided by the National Science Foundation (NSF) (CHE-1465263 to V.M.D. and CHE-1565669 to O.W.). D.N.L. is grateful for an NSF Graduate Fellowship. We acknowledge Yamin Zhu (Shanghai Jiao Tong University) for help with substrate synthesis and the Nowick lab for use of HPLC instrumentation.

References

1. Rebek J. Molecular recognition with model systems. *Angew. Chem. Int. Ed* 29, 245–255 (1990).
2. Milton RC, Milton SC & Kent SB Total chemical synthesis of a D-enzyme: the enantiomers of HIV-1 protease show reciprocal chiral substrate specificity. *Science* 256, 1445–1448 (1992). [PubMed: 1604320]
3. Koeller KM & Wong C-H Enzymes for chemical synthesis. *Nature* 409, 232–240 (2001). [PubMed: 11196651]
4. Steitz TA From the structure and function of the ribosome to new antibiotics. *Angew. Chem. Int. Ed* 49, 4381–4398 (2010).
5. Ramakrishnan V. Unraveling the structure of the ribosome. *Angew. Chem. Int. Ed* 49, 4355–4380 (2010).
6. Yonath A. Hibernating bears, antibiotics, and the evolving ribosome. *Angew. Chem. Int. Ed* 49, 4340–4354 (2010).
7. Clancy S & Brown W. Translation: DNA to mRNA to Protein. *Nature Education* 1, 101 (2008).
8. Steitz TA A structural understanding of the dynamic ribosome machine. *Nat. Rev. Mol. Cell Biol* 9, 242–253 (2008). [PubMed: 18292779]
9. Lewandowski B. et al. Sequence-specific peptide synthesis by an artificial small-molecule machine. *Science* 339, 189–193 (2013) [PubMed: 23307739]
10. Fogg DE & dos Santos EN Tandem catalysis: a taxonomy and illustrative review. *Coord. Chem. Rev* 248, 2365–2379 (2004).
11. Kuzin AP, Sun T, Jorczak-Baillass J, Healy VL, Walsh CT & Knox JR Enzymes of vancomycin resistance: the structure of D-alanine–D-lactate ligase of naturally resistant *Leuconostoc mesenteroides*. *Structure* 8, 463–470 (2000). [PubMed: 10801495]

12. Álvarez R, López Cortés LE, Molina J, Cisneros JM & Pachón J. Optimizing the Clinical Use of Vancomycin. *Antimicrob. Agents Chemother* 60, 2601–2609 (2016). [PubMed: 26856841]
13. Craik DJ Seamless proteins tie up their loose ends. *Science* 311, 1563–1564 (2006). [PubMed: 16543448]
14. Fairlie DP, Abbenante G & March DR Macrocyclic peptidomimetics - forcing peptides into bioactive conformations. *Curr. Med. Chem* 2, 654–686 (1995).
15. Carlos M-M, Florian R & Horst K. Cilengitide: The first anti-angiogenic small molecule drug candidate. Design, synthesis and clinical evaluation. *Anticancer Agents Med. Chem* 10, 753–768 (2010). [PubMed: 21269250]
16. White CJ & Yudin AK Contemporary strategies for peptide macrocyclization. *Nat. Chem* 3, 509–524 (2011). [PubMed: 21697871]
17. Merrifield B. Solid phase synthesis. *Science* 232, 341 (1986). [PubMed: 3961484]
18. Davies JS The cyclization of peptides and depsipeptides. *J. of Pept. Sci* 9, 471–501 (2003). [PubMed: 12952390]
19. Le DN, Riedel J, Kozlyuk N, Martin RW & Dong VM Cyclizing pentapeptides: Mechanism and application of dehydrophenylalanine as a traceless turn-inducer. *Org. Lett* 19, 114–117 (2017). [PubMed: 27973857]
20. Doherty DG, Tietzman JE & Bergmann M. Peptides of dehydrogenated amino acids *J. Biol. Chem* 147, 617–637 (1943).
21. Fernandez-Lopez S. et al. Antibacterial agents based on the cyclic D,L- α -peptide architecture. *Nature* 412, 452–455 (2001). [PubMed: 11473322]
22. Goldberg J. Cyclic peptide antibiotics; self-assembly required. *Trends Biotechnol* 19, 379 (2001).
23. Halpern J. Mechanism and stereoselectivity of asymmetric hydrogenation. *Science* 217, 401–407 (1982). [PubMed: 17782965]
24. Donoghue PJ, Helquist P, Norrby P-O & Wiest O. Development of a Q2MM force field for the asymmetric rhodium catalyzed hydrogenation of enamides. *J. Chem. Theory Comput* 4, 1313–1323 (2008). [PubMed: 26631706]
25. Hansen E, Rosales AR, Tutkowski B, Norrby P-O & Wiest O. Prediction of stereochemistry using Q2MM. *Acc. Chem. Res* 49, 996–1005 (2016). [PubMed: 27064579]
26. Donoghue PJ, Helquist P, Norrby P-O & Wiest O. Prediction of enantioselectivity in rhodium catalyzed hydrogenations. *J. Am. Chem. Soc* 131, 410–411 (2009). [PubMed: 19140780]
27. Weiss MS, Jabs A & Hilgenfeld R. Peptide bonds revisited. *Nat. Struct. Mol. Biol* 5, 676–676 (1998).
28. Tang W, Jiménez-Osés G, Houk KN & van der Donk WA Substrate control in stereoselective lanthionine biosynthesis. *Nat. Chem* 7, 57–64 (2015). [PubMed: 25515891]
29. Tang W & Zhang X. New chiral phosphorus ligands for enantioselective hydrogenation. *Chem. Rev* 103, 3029–3070 (2003). [PubMed: 12914491]
30. Liu D & Zhang X. Practical P-chiral phosphane ligand for Rh-catalyzed asymmetric hydrogenation. *Eur. J. Org. Chem* 2005, 646–649 (2005).
31. Osberger TJ, Rogness DC, Kohrt JT, Stepan AF & White MC Oxidative diversification of amino acids and peptides by small-molecule iron catalysis. *Nature* 537, 214–219 (2016). [PubMed: 27479323]
32. van Dongen SFM, Elemans JAAW, Rowan AE & Nolte RJM Processive catalysis. *Angew. Chem. Int. Ed* 53, 11420–11428 (2014).
33. Knowles WS & Sabacky MJ Catalytic asymmetric hydrogenation employing a soluble, optically active, rhodium complex. *Chemical Communications (London)*, 1445–1446 (1968).
34. Noyori R. et al. Asymmetric synthesis of isoquinoline alkaloids by homogeneous catalysis. *J. Am. Chem. Soc* 108, 7117–7119 (1986).
35. Meyer D. et al. Stereoselective synthesis of dipeptides by asymmetric reduction of dehydropeptides catalyzed by chiral rhodium complexes. *J. Org. Chem* 45, 4680–4682 (1980).
36. Vigneron JP, Dhaenens M & Horeau A. Nouvelle methode pour porter au maximum la purete optique d'un produit partiellement dedouble sans l'aide d'aucune substance chirale. *Tetrahedron* 29, 1055–1059 (1973)

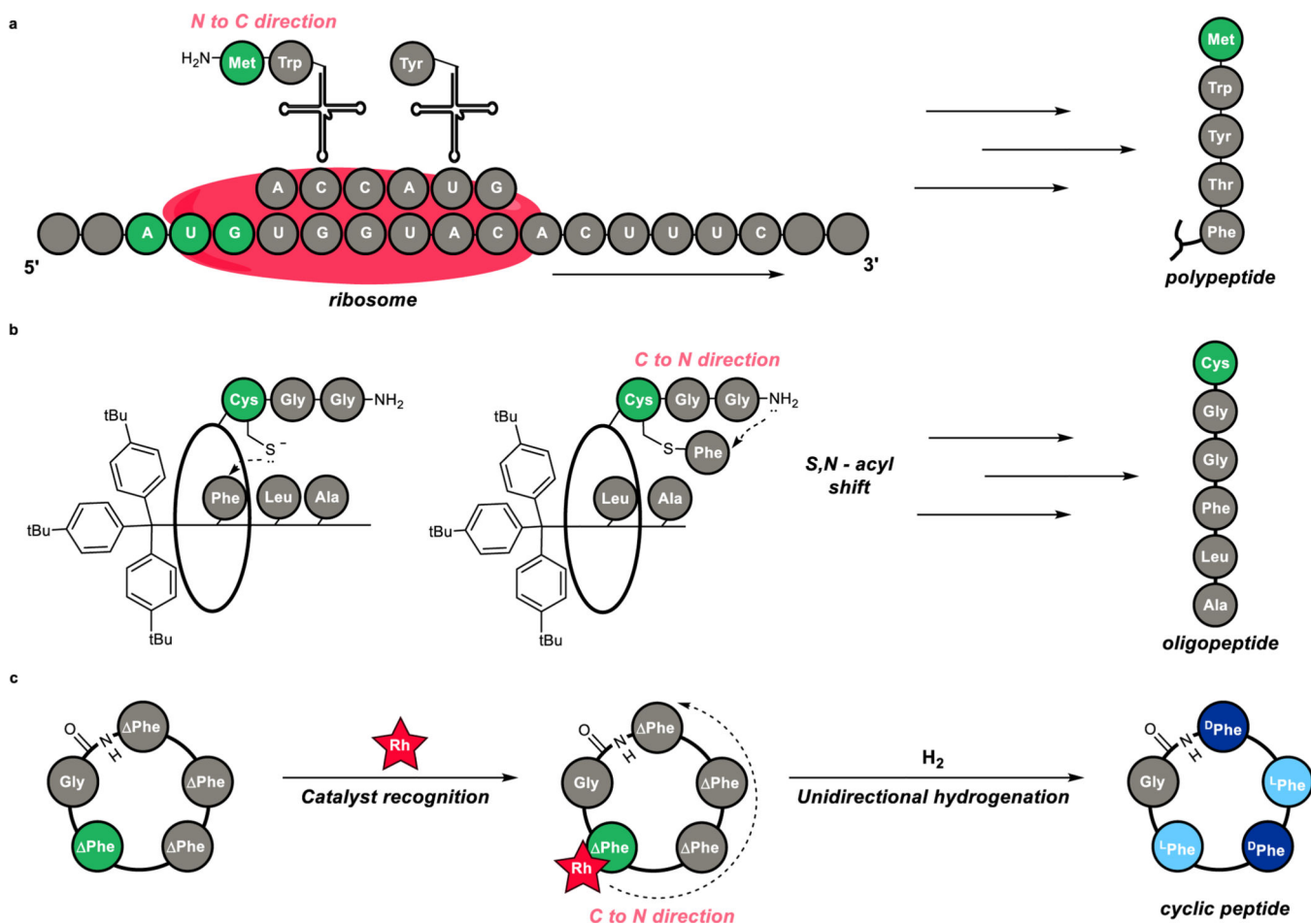


Figure 1. Unidirectional peptide synthesis is catalyzed by enzymes and synthetic catalysts.
a. Sequence recognition by ribosomes enables peptide synthesis (in nature). **b.** Synthetic rotaxane enables directional peptide synthesis (Leigh, 2013). **c.** Molecular recognition of dehydrophenylalanine enables unidirectional cascade reduction (this work).

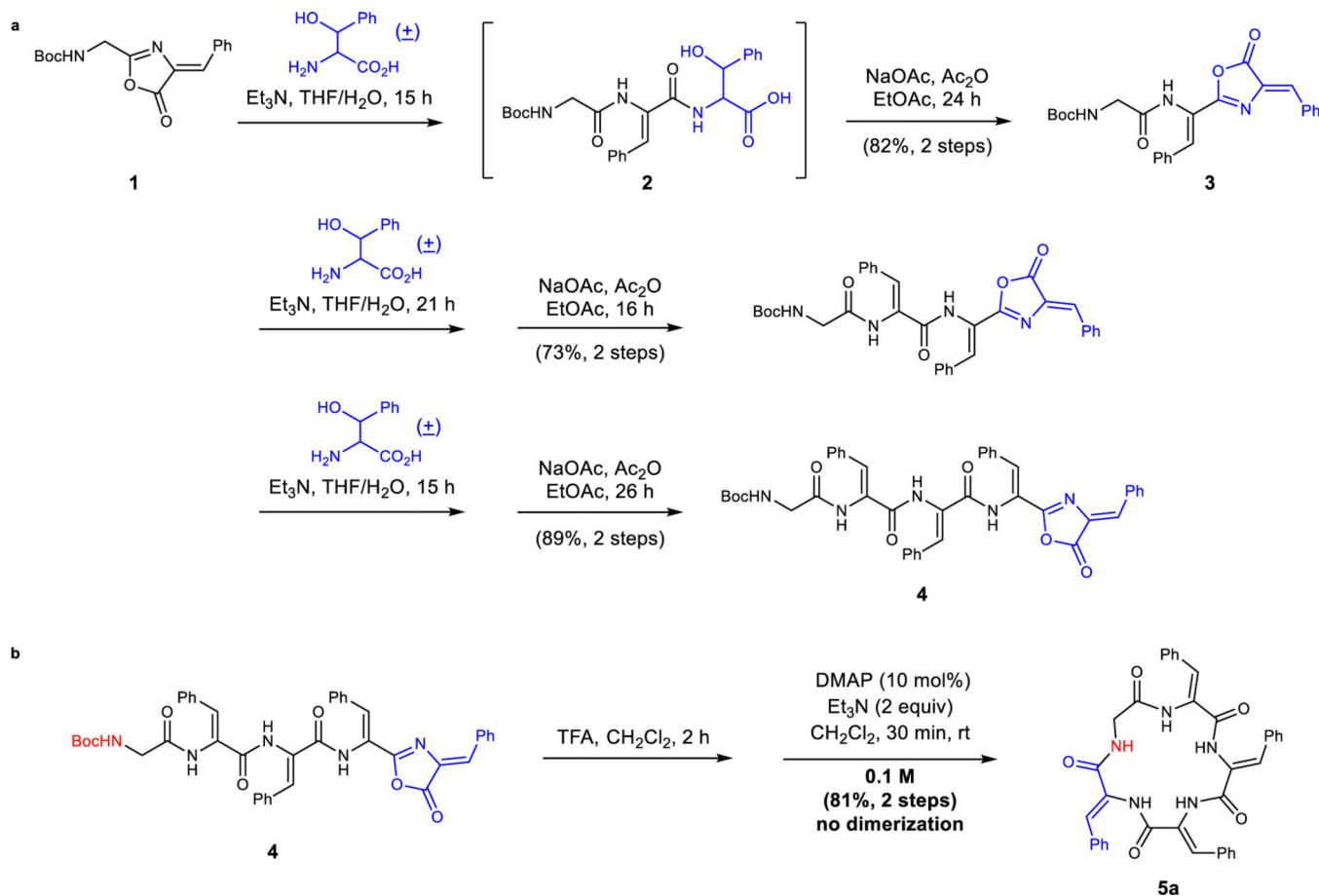


Figure 2. Synthesizing cyclic dehydropeptides using dehydroamino acids.

a, Synthesis and elongation of linear dehydropeptide is enabled using oxazolones and (\pm) - β -phenylserine. **b**, Macrocyclization of linear dehydropeptides proceeds at high concentration. Boc, *t*-butyloxycarbonyl; TFA, trifluoroacetic acid; DMAP, 4-dimethylaminopyridine; rt, room temperature.

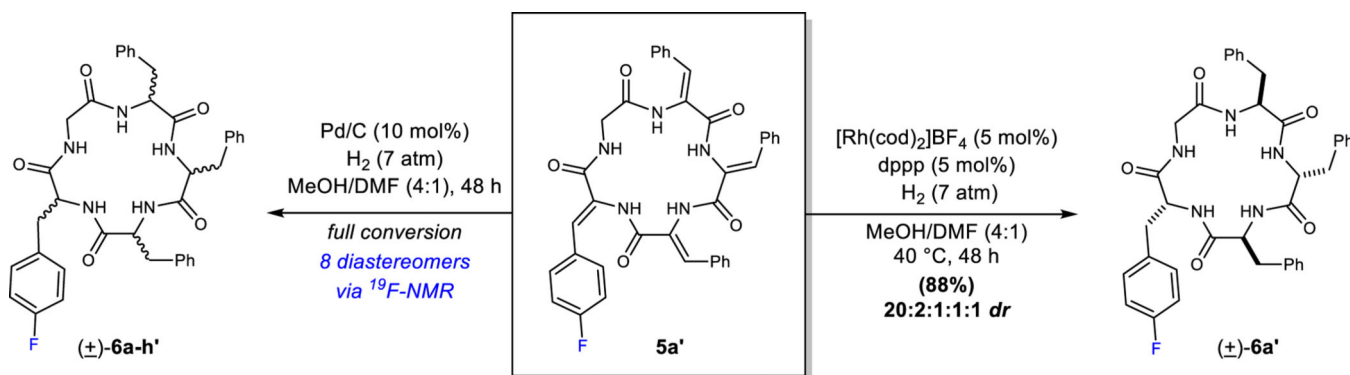


Figure 3. Examining the hydrogenation of cyclic dehydropeptide **5a' gives mechanistic insight.** Pictured on the left is the hydrogenation of cyclic dehydropeptide **5a'** using heterogeneous catalysis. Shown on the right is the hydrogenation of cyclic dehydropeptide **5a'** using achiral rhodium catalysis. cod, 1,5-cyclooctadiene; dppp, 1,3-bis(diphenylphosphino)propane; atm, atmosphere. The inclusion of a prime in the compound number indicates it is the fluorinated analog. *E.g.* **5a** = cyclo(Gly- Phe- Phe- Phe- Phe) **5a'** = cyclo(Gly- Phe- Phe- Phe- Phe(4-F)), Phe, dehydrophenylalanine.

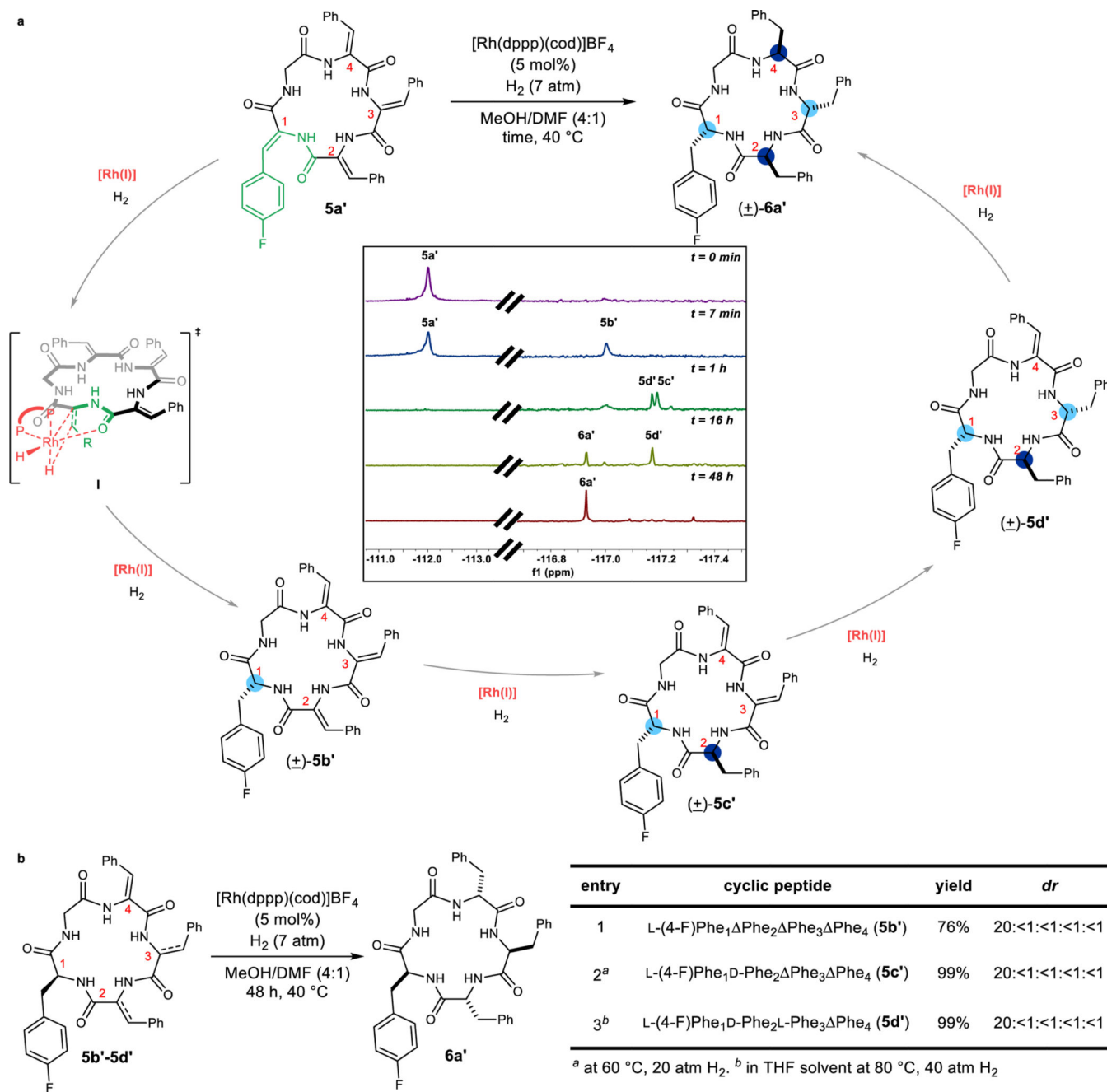


Figure 4. Mechanistic experiments support a unidirectional hydrogenation.

a, ^{19}F -NMR time trace supports sequential reduction. **b**, Subjecting the synthesized intermediates to standard hydrogenation conditions yields cyclic peptide **6a'** with high diastereoselectivity.

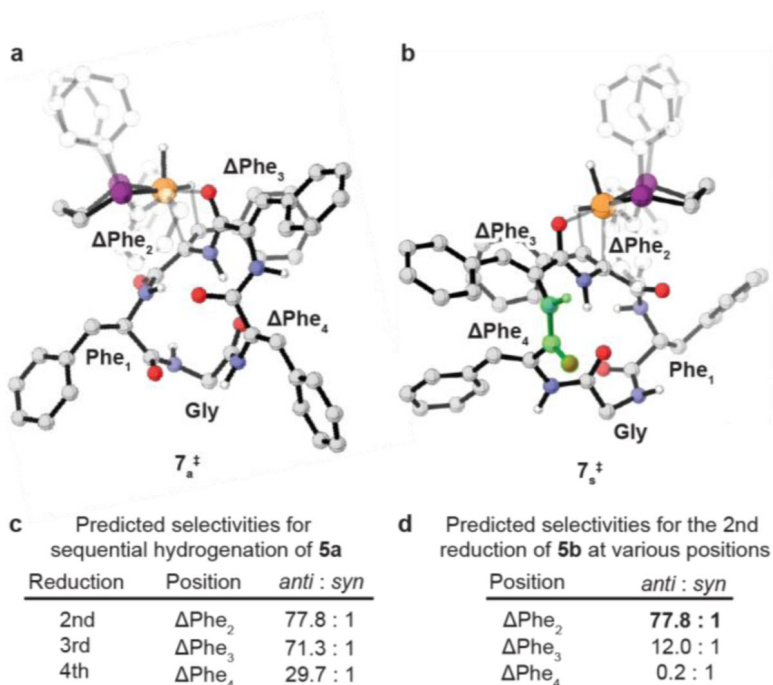


Figure 5. Computational support for a sequential and unidirectional cascade reduction (Non-reacting hydrogens have been hidden and phenyls on the ligand are shown transparent for clarity).

a, Lowest energy transition structure 7_s^\ddagger for hydrogenation at Phe_2 leading to the *anti* diastereoselectivity. **b**, Lowest energy transition structure 7_s^\ddagger for hydrogenation at Phe_2 leading to the *syn* diastereoselectivity. **c**, Predicted selectivities for hydrogenation supports sequential reduction. **d**, Predicted selectivities support second diastereoselective reduction occurring at Phe_2 while a reduction occurring at Phe_3 or Phe_4 would lead to diminished diastereoselectivity. **5b** = cyclo(Gly- Phe- Phe- Phe-Phe)

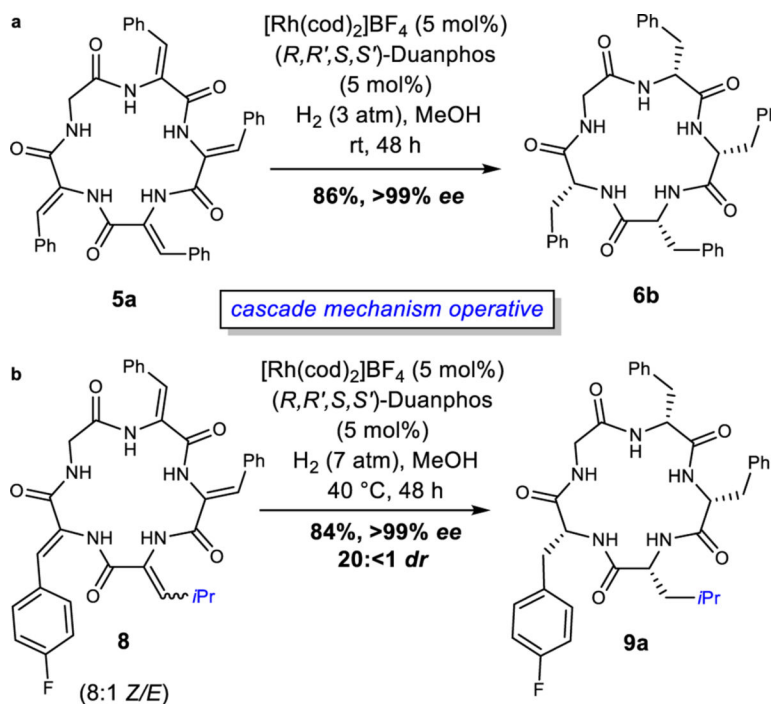


Figure 6. Cascade hydrogenation of cyclic dehydropeptide **5a** and **8** using chiral Rh catalysis yields a different result.

a, Duanphos ligand overcomes substrate control to generate homochiral peptide with high selectivity via cascade hydrogenation. **b**, Cascade hydrogenation is extended to cyclic dehydropeptide **8**.